Astronomy
&
Astrophysics

The secrets of T Pyxidis

I. UV observations[*]

R. Gilmozzi[1] and P. Selvelli[2]

[1] European Southern Observatory, Karl-Schwarzschild-Str. 2, 85748 Garching, Germany
e-mail: rgilmozz@eso.org
[2] INAF - Osservatorio Astronomico di Trieste, via Tiepolo 11, 34143 Trieste, Italy
e-mail: selvelli@oats.inaf.it

ABSTRACT

Aims. We study the UV spectral behavior of the recurrent nova T Pyx during 16 years of *IUE* observations.
Methods. We examined both the *IUE* line-by-line images and the extracted spectra in order to understand the reality and the origin of the observed spectral variations. We compare different extraction methods and their influence on the spectrum of an extended object.
Results. The UV continuum of T Pyx has remained nearly constant in slope and intensity over this time interval, without any indication of long-term trends. The reddening determined from the UV data is $E_{B-V} = 0.25 \pm 0.02$. The best single-curve fit to the dereddened UV continuum is a power-law distribution $\propto \lambda^{-2.33}$. The tail of this curve agrees well with the *B*, *V*, and *J* magnitudes of T Pyx, indicating that the contribution of the secondary star is negligible. One peculiar aspect of T Pyx is that most emission lines (the strongest ones being those of CIV 1550 and HeII 1640) show substantial changes both in intensity and detectability, in contrast to the near constancy of the continuum. Several individual spectra display emission features that are difficult to identify, suggesting a composite spectroscopic system. We tentatively ascribe the origin of these transient emission features either to loops and jets from the irradiated secondary or to moving knots of the surrounding nebula that are (temporarily) projected in front of the system. The inspection of all IUE line-by-line images has led to the detection of emission spikes *outside* the central strip of the spectrum, which in some cases seem associated to known emission features in the (main) spectrum. A comparison with other ex-novae reveals a surprising similarity to the spectrum of the very-slow nova HR Del, whose white dwarf primary has a mass that is allegedly about one half that of T Pyx.

Key words. stars: novae, cataclysmic variables – ultraviolet: stars

1. Introduction

The five recorded outbursts of the recurrent nova (RN) T Pyx occurred in 1890, 1902, 1920, 1944, and 1966, with a mean recurrence time of 19 ± 5.3 yrs (Webbink et al. 1987, hereinafter WLTO). All outbursts were remarkably similar in photometric behavior and characterized by a speed class that was substantially slower than in other RNe, with $t_2 = 60^d$ instead of a few days. We note that according to the classifications of Payne-Gaposchkin (1957) and Warner (1995) T Pyx should be considered "moderately fast" and not "extremely slow" as reported in previous works.

It is unfortunate that the orbital period of the binary system has not been clearly established. The published results range from values as low as 1^h40^m (Szkody & Feinswog 1988, from a single sine solution of J photometry) to values as high as 3^h29^m (Vogt et al. 1989, from a preliminary study of spectroscopic data with limited spectral resolution). A more recent and comprehensive photometric study by Schaefer et al. (1992) based on data from 114 nights of observations, together with measurements from the literature, has led to the disappointing conclusion that T Pyx has an incoherent photometric period and that the sinusoidal modulation is not closely tied to the orbital period. By analogy with other stars that have variable photometric periods

(possibly related to the superhump phenomenon), Shaefer et al. (1992) suggested an orbital period of near 1^h45^m from the "best" period for the modulation (1^h49^m). The relation between the orbital periods of cataclysmic variables and the spectral types of the secondary stars (Smith and Dhillon 1998) indicates that the secondary star in T Pyx is probably an M 4–5 dwarf.

Already in 1979 ground-based imaging by Duerbeck & Seitter (1979) detected a shell of ejected matter, a few arcsec across, that surrounded the system. Subsequent observations by Seitter (1986) and Duerbeck (1987) revealed the presence of structures in the shell, while Shara et al. (1989) discovered the additional presence of a fainter extended shell with a radius of about 10 arcsec. Thanks to the high spatial resolution of the WFPC2 on board the HST, the "shell" has been resolved into more than two thousand individual knots (Shara et al. 1997).

These observations have provided direct evidence that the ejecta of novae, previously believed to be reasonably homogeneous, are instead highly structured, confirming the GHRS observations by Shore et al. (1993) that established the presence of knots in Nova Cyg 1992 and the indirect conjectures on the existence of knots previously made by Krautter et al. (1984), Williams et al. (1991), and Saizar & Ferland (1994).

Shabbaz et al. (1997) interpreted the presence of two spectral features on either side of Hα as the signature of a bi-polar, high-velocity, highly collimated jet, but subsequent studies by Margon & Deutsch (1998) and by O'Brien & Cohen (1998) have shown

---

[*] Based on observations made with the International Ultraviolet Explorer and de-archived from the ESA VILSPA Database.
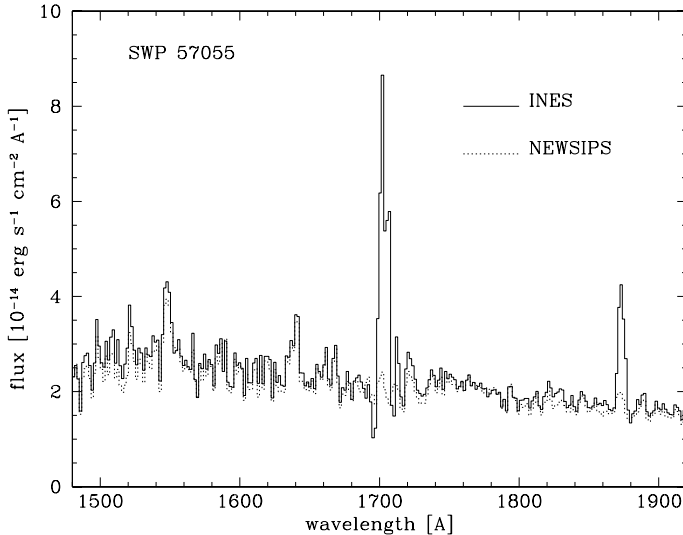
Fig. 1. Comparison of NEWSIPS and INES extraction methods. Note the two strong lines near 1703 and 1873 Å present only in the INES extraction.

that these features are instead emission in the [NII] 6548 and 6584 lines from a complex velocity field in the surrounding shell.

1.1. The missing outburst

Observations of an RN for which an outburst is expected to occur provide a unique opportunity for a direct observational test of the theoretical expectations of the thermonuclear runaway (TNR) theory. >From the observed $\dot{M}$ and the inter-outburst interval, one can indeed estimate the total accreted mass M_{accr} and compare it to both the theoretical mass for ignition M_{ign} and the observed mass of the ejected shell M_{ej}. Ultraviolet observations are best-suited for these studies since most of the accretion disk luminosity is emitted in the far-UV and many emission lines of important astrophysical species are present in this wavelength range.

With this rationale in mind and in view of the allegedly imminent outburst of T Pyx, as expected on the basis of its apparently regular behavior, with a mean interval of about 19 years between the observed outbursts (WLTO), and of the about twenty years elapsed from the last outburst of December 1966, we started an observing program in 1986 with *IUE* with the purpose of monitoring the quiescent phase and to follow the spectroscopic changes in the phases prior to the outburst and during the early outburst. Actually, the star has successfully managed to postpone the long-awaited outburst, and at the present time (2006) has surpassed by sixteen years the longest inter-outburst interval so far recorded (24 yr).

Shortly before this paper neared completion, Schaefer (2005) published the results of a study on the interoutburst interval in recurrent novae. >From an analysis of the data on the magnitudes obtained from archival plates, from the literature, and from his own collection of CCD magnitudes, he found that the product of the inter-eruption interval times the average bolometrically corrected flux is a constant for both T Pyx and U Sco. This finding, together with the apparent decline in the observed B magnitude in the last inter-eruption intervals (Fig. 1 in Shaefer's paper), has provided a physical basis for predicting that the next outburst of T Pyx will occur around 2052.

While waiting to (hopefully) personally verify these predictions, we present and discuss here (Paper I) the main spectroscopic results from 16 years of *IUE* observations. In a follow-up paper (Selvelli & Gilmozzi 2006, Paper II), we will combine the results of these observations with other basic information on the system (including the implications of the findings by Schaefer 2005, on the accretion rate of T Pyx during the past inter-eruption intervals), in order to set stringent constraints on the physical parameters of this elusive object and to refine our understanding of the recurrent nova phenomenon.

2. The IUE observations and data reduction

The only *IUE* observations of T Pyx previous to ours were those of May 11, 1980 by Seitter and Duerbeck and reported by Bruch et al. (1981). In this preliminary study they found $E_{B-V} \sim 0.35$ and gave an estimate for the distance of about 2500 pc.

The *IUE* spectra cover the time interval from May 11, 1980 to May 7, 1996 (with a gap between 1980 and 1987). In total, 37 short wavelength (SWP camera) and 14 long wavelength (LWP camera) spectra are available, although some SWP spectra present a low S/N because of high background noise and/or a bad photometric response as a consequence of unusual centering in the *IUE* aperture. Typical exposure times for the SWP spectra were around three hours with a few exposures twice as long (Table 1).

An important aspect of data reduction is that the *IUE* data extraction and calibration methods have undergone several revisions during and after the *IUE* lifetime, which has led to a general improvement in the quality of the line spectrum. While this work was in progress (from 1987 to the last spectra secured in May 1996), both the IUESIPS and then NEWSIPS extraction procedures were adopted. See Gilmozzi et al. (1998) for some considerations of the difference in the quality of data extraction using IUESIPS or NEWSIPS.

The spectra used in this paper were instead retrieved from the INES (*IUE* Newly Extracted Spectra) final archive. The more relevant modifications in the INES system, in comparison with NEWSIPS, are: 1) the adoption of a new noise model; 2) a more accurate representation of the spatial profile of the spectrum; 3) a more reliable determination of the background; 4) a more adequate treatment of "bad" pixels; and 5) the improvement in the handling and propagation of the quality flags to the final extracted spectra. In general, the extracted fluxes of INES and NEWSIPS are in excellent agreement, but especially for spectra with weak continua and narrow emission lines the INES extraction can register significantly more flux (up to ten sigma!) (Schartel and Skillen 1998). For a detailed description of the *IUE*-INES system see Rodriguez-Pascual et al. (1999) and Gonzalez-Riestra et al. (2001).

For T Pyx, a comparison between the NEWSIPS and INES extraction methods of the *same* spectrum has shown in several cases remarkable differences in the strength of some emission features. Figure 1 (SWP57055) is an outstanding example of this problem that may surely help to emphasize the difficulties we have had in assessing the reality of some spectral features. The features at 1703 and 1873 Å in the INES extracted spectrum are due to knots of emission located outside the strip that defines the spectrum (they are flagged as "cosmic rays" but that they are quite wide and both lie at exactly the same distance from the spectrum might indicate that they may be real spectral features originating from an extended region, see also Fig. 6). While NEWSIPS automatically removes these lines (with the

Table 1. *IUE* observation log.

Camera	Image	Date	ExpTime [s]	Comments
LWR	07724	1980-05-11	7199.8	
SWP	08973	1980-05-11	12899.8	
LWP	09204	1986-09-27	7199.8	
SWP	29318	1986-09-27	16199.5	
SWP	32218	1987-11-02	16799.6	
LWP	11996	1987-11-02	6599.7	
LWP	12644	1988-02-11	7199.8	
SWP	32899	1988-02-11	12779.8	
LWP	12791	1988-03-03	12779.8	
SWP	33034	1988-03-04	23579.7	
LWP	14383	1988-11-05	7799.4	
SWP	34696	1988-11-05	17159.6	
LWP	16757	1989-11-07	7799.4	
SWP	37536	1989-11-07	16799.6	
SWP	43442	1991-12-22	15599.4	
LWP	22052	1991-12-22	7199.8	
SWP	44182	1992-03-16	14999.8	
LWP	22608	1992-03-16	9599.6	
SWP	44948	1992-06-17	16799.6	
LWP	23317	1992-06-18	6899.5	
LWP	24612	1992-12-28	8399.5	
SWP	46605	1992-12-28	16319.5	
SWP	47057	1993-02-27	16499.7	
LWP	25020	1993-02-27	6599.7	
SWP	47323	1993-03-20	20099.7	poor center
SWP	47328	1993-03-21	17999.7	poor center
SWP	47332	1993-03-22	23099.6	
SWP	49365	1993-11-29	9599.6	noisy
SWP	49366	1993-11-29	10679.7	noisy
SWP	50099	1994-02-24	11399.8	
SWP	50100	1994-02-24	10799.7	noisy
SWP	50596	1994-04-20	24479.6	
SWP	52886	1994-11-23	8999.6	
SWP	52887	1994-11-23	9479.6	noisy
SWP	53809	1995-02-02	11399.8	
SWP	53810	1995-02-02	10679.7	noisy
SWP	54590	1995-05-03	11099.6	
SWP	54591	1995-05-04	11699.6	noisy
SWP	56240	1995-11-26	11999.5	
SWP	57030	1996-05-01	11999.5	
SWP	57031	1996-05-02	12599.5	
SWP	57032	1996-05-02	11999.5	
SWP	57033	1996-05-03	11999.5	
SWP	57034	1996-05-03	10799.7	
SWP	57035	1996-05-03	6599.7	
SWP	57039	1996-05-04	7799.4	
SWP	57042	1996-05-04	9899.4	
SWP	57047	1996-05-05	10799.7	
LWP	32286	1996-05-05	5699.8	
SWP	57055	1996-05-06	10799.7	
LWP	32287	1996-05-06	6599.7	

Fig. 2. Average *IUE* spectrum of T Pyx obtained by co-adding and merging 35 SW and 14 LW IUE spectra. *Top*: observed, *bottom*: dereddened with $E_{B-V} = 0.25$ (this paper).

calibration tables have had on the shape of the continuum and consequently on the depth of the interstellar absorption bump. In turn, this has resulted in non negligible changes in our estimates of the reddening and of the UV-integrated flux and consequently on the distance, the UV luminosity, and ultimately the mass accretion rate (see Paper II).

3. The continuum energy distribution

The observed UV continuum distribution of T Pyx has remained nearly constant in slope and intensity over the 16 years of *IUE* observations showing only minor variations and no indication of any long term trends. In the SWP region the standard deviation is only 3.7%, even including the badly exposed spectra. This has justified the creation of an average spectrum (Fig. 2, top) by co-adding and merging all SWP and LW spectra that are not underexposed or badly centered.

The improved S/N in the average spectrum has allowed both the detection of weak line features and an accurate determination of the reddening. We obtained $E_{B-V} = 0.25 \pm 0.02$ by the standard method of removing the broad interstellar extinction feature centered at 2175 Å using the average interstellar absorption curve of Savage and Mathis (1978). Therefore in the present study and in Paper II we adopt $A_v = 3.15 \times 0.25 \sim 0.78$. The same method applied earlier to the smaller sample of spectra processed with IUESIPS gave $E_{B-V} = 0.31$, while for NEWSIPS spectra it gave $E_{B-V} = 0.24$.

One should note that there is some confusion in the literature about the E_{B-V} value for T Pyx: WLTO used the preliminary

risk of removing also real emission features), INES is more conservative and keeps the features but puts a proper quality flag in the corresponding spectrum column. In view of these problems that are especially critical when one deals with the spectrum of an object that is surrounded by an extended shell, we have carefully checked all line-by-line (SILO) images for the presence of similar pseudo-emission features in order to guarantee the reality of the emission features that are present in the various INES extracted spectra (see also Sect. 4.2).

Another non minor consequence of the migration from IUESIPS to NEWSIPS and finally to INES is in the effects that the changes in the extraction methods and in the absolute
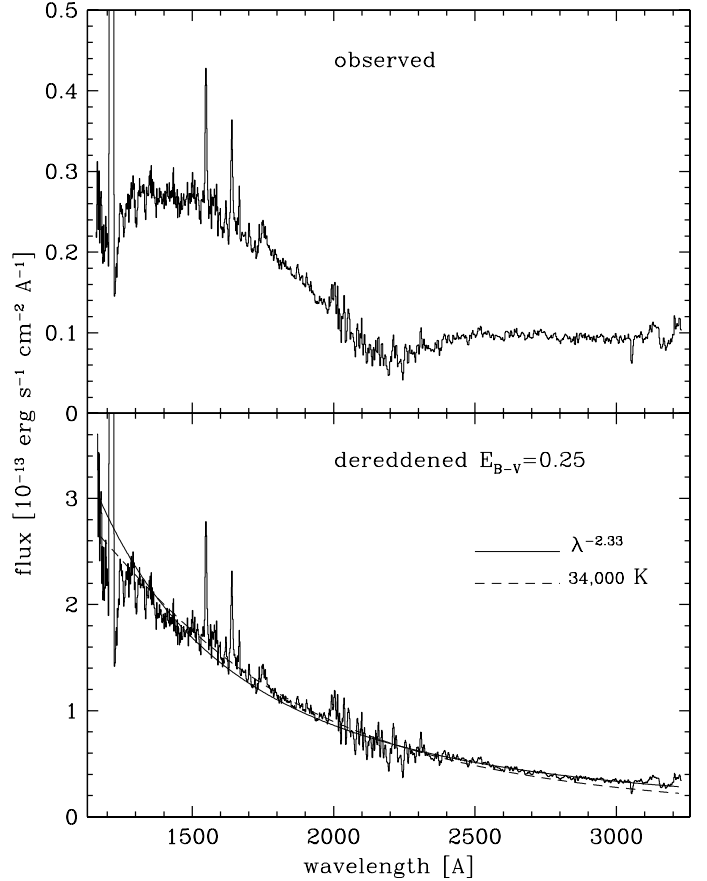
value $E_{B-V} = 0.35$ by Bruch et al. (1981, but they reported it as 0.36) and therefore obtained dereddened colors $(B-V)_o = -0.26$ and $(U - B)_o = -1.25$, which look too negative. These same colors were subsequently adopted by Patterson et al. (1998), who on this basis concluded that "T Pyx is the bluest nova remnant in the sky". Bruch and Engel (1994) reported $E_{B-V} = 0.20$ and $(B - V) = 0.14$ from which they derived $(B - V)_o = -0.06$. (This $E_{B-V} = 0.20$ value is probably a typo, because they give Bruch et al. 1981, as a reference, but, unfortunately, this same value was listed also by Szkody 1994). Finally, Weight et al. (1994) gave $E_{B-V} = 0.08$ in a near-IR study of old classical novae.

The UV continuum is clearly defined longwards of 1400 Å where only a few and well-known emission lines are present in the SWP spectra, while the LW region is poorer in line features. For a correct positioning of the continuum in the region below 1400 Å, where it was not clear whether the spectral features were actually in absorption or in emission, we have been helped by a preliminary identification of these line features (most of them come out as absorption lines, see Sect. 5). The presence of a wide interstellar or circumstellar Lyα absorption, which extends longward up to 1250 Å, together with that of the strong Lyα emission of geocoronal origin has also made it rather difficult to estimate the continuum below 1260 Å. Therefore, we first determined the continuum in the range 1260–3200 Å using only line-free regions, fitted it with a spline, and extrapolated it to shorter wavelengths. A less interactive fitting method (the *icfit* task in IRAF) yielded a very similar result.

The best single-curve fit to the UV continuum is a power-law distribution $F_\lambda = 4.28 \, 10^{-6} \, \lambda^{-2.331}$ (erg cm^{-2} s^{-1} Å^{-1}), with a small uncertainty of ± 0.04 in the index. This spectral index is exactly the Lynden-Bell law for a standard disk ($\alpha = -2.33$). A black body with $T = 34\,160$ K is also a good fit, although it would be difficult to ascribe a single temperature to the most plausible source of the continuum, the accretion disk. The lower half of Fig. 2 shows a plot of the dereddened average spectrum together with the continuum fits (see also Fig. 8). The $\lambda\lambda$ 1180–3230 integrated flux of both the reddening-corrected average continuum and the power-law fit is 1.94×10^{-10} erg cm^{-2} s^{-1}.

4. The emission line spectrum

The strongest emission features are CIV 1550 and HeII 1640 (Fig. 3, top), while weaker emission lines are identified as OIII] 1666, NIII] 1750, etc. (see Table 2 for a list of additional emission lines in the average spectrum, together with their tentative identification and their reddening-corrected emission intensity). The LW region seems almost featureless, but a closer inspection reveals marginal evidence of weak emission and absorption features. The emission line near 3135 Å is identified as OIII 3134, a Bowen fluorescence line excited by the HeII Ly-α transition at 303.8 Å.

An examination of the individual spectra shows that only the emission lines of CIV 1550 and HeII 1640 are present in all spectra, although quite variable, while OIII] 1666 and NIII] 1750 are present in about one half of the spectra. The changes in intensity of the emission lines of CIV 1550 and HeII 1640 are associated to changes in the line width. Table 3 gives the observed equivalent width (*EW*) and *FWHM* for these emission lines, although the limited spectral resolution of the data has precluded very accurate measurements. A good correlation (rms of residuals =1.015) exists between the *FWHM* and the *EW* of the HeII 1640 line (Fig. 4). The corresponding correlation for the CIV 1550 emission line is poorer (rms of residuals =1.579),
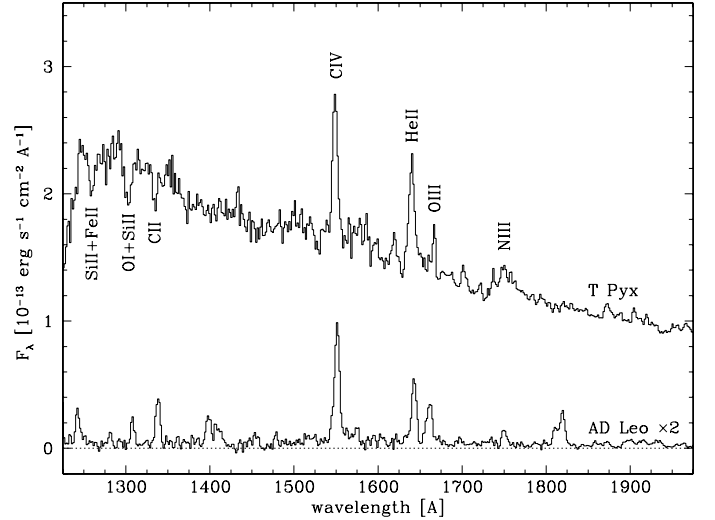

Fig. 3. Details of the dereddened average spectrum of T Pyx in the SW range. The spectrum of the late-type active star AD-Leo (*bottom*) is included for comparison (see Sect. 6.2).

Table 2. The intensities of the emission lines in the average spectrum and their proposed identifications.

Wavelength[a] (Å)	Intensity (10^{-13} erg cm^{-2} s^{-1})	Identification[b]
1177	1.98	CIII(4) 75.70
1291	1.02	CI(4.01) 87.82 ?
1354	0.50	OI(1) 55.60 + CI(43) 54.28 + CI(42) 55.84
1433	0.62	unidentified (also in HR Del)
1502	0.73	SiIII 1501 (diel.) ?
1510	0.41	OV(64) 06.76 ?
1520	0.37	unidentified
1550	8.35	CIV(1) 49.50
1565	0.62	CI(UV3) 60.86 ?
1578	0.72	CIII(UV12.03) 77.25 ?
1586	0.93	OIII(19.23) 87.53 ?
1620	0.72	(CIII(11.72) 20.30 + NV(53) 19.74) ?
1640	6.32	HeII(12) 1640.39
1667	1.26	OIII(0.01) 64.15
1702	0.22	OV(67) 07.99 ?
1738	0.30	NII(13.25) 42.25 ?
1750	2.32	NIII(0.01) 50.46
1872	0.63	unidentified
1905	0.35	CIII(0.01) 06.67
1920	0.16	CIII(12.02) 23.13 ?
2308	1.22	HeII(Pa) 06.20 + ?
2392	0.37	HeII(Pa) 85.40 ?
2516	0.74	HeII(Pa) 11.21 ? + ?
2733	0.41	HeII(Pa) 33.32
3134	1.84	OIII(12) 32.79 (Bowen)

[a] The listed wavelength is the mean multiplet wavelength; [b] identifications marked with a (?) are doubtful.

while the correlation between the fluxes in the HeII 1640 and CIV 1550 lines is just fair.

4.1. The emission lines present in individual spectra only

One peculiar aspect of the line spectrum of T Pyx is that the emission lines show substantial changes in intensity and detectability in the individual spectra, in sharp contrast to the near

Table 3. The equivalent widths (*EW*) and *FWHM* for the emission lines of CIV 1550 and HeII 1640 in individual spectra.

| SWP | CIV 1550 | | HeII 1640 | |
	FWHM [Å]	*EW* [Å]	*FWHM* [Å]	*EW* [Å]
08973	11.6	6.7	6.8	4.7
29318	3.7	6.4	6.3	5.8
32218	6.2	4.4	5.6	4.8
32899	6.0	5.5	8.3	6.1
33034	6.4	11.5	6.0	4.6
34696	5.1	4.9	5.0	4.4
37536	5.0	4.1	7.6	4.0
43442	7.8	5.6	4.2	2.1
44182	6.3	4.5	4.9	3.0
44948	7.4	5.5	3.3	2.2
46605	5.8	3.6	13.7	11.8
47057	7.0	4.5	4.9	3.6
47323	6.4	3.9	4.2	2.8
47328	6.7	4.8	8.2	3.7
47332	5.4	4.1	8.3	7.5
49365	8.6	6.9	9.5	6.6
49366	7.8	5.5	7.9	4.3
50099	6.5	4.0	5.5	2.3
50100	5.	3.6	8.3	7.5
50596	6.3	4.3	7.7	5.9
52886	4.0	4.4	5.5	2.8
52887	4.5	4.4	5.4	2.9
53809	6.1	4.8	8.3	6.2
53810	7.3	5.8	5.7	2.7
54590	10.2	4.6	9.5	4.6
56240	8.7	6.6	4.6	1.8
57030	6.3	6.6	5.7	3.2
57031	5.9	5.2	8.0	4.6
57032	6.1	5.0	5.8	3.7
57033	6.0	6.1	6.1	3.7
57034	6.7	6.9	5.6	2.5
57035	7.1	8.4	7.6	6.2
57039	5.6	4.8	3.6	0.9
57042	4.0	4.1	5.5	2.1
57047	3.1	2.0	8.0	6.2
57055	5.7	4.4	4.6	2.4

Fig. 4. Correlation between the *FWHM* and the equivalent width for the HeII 1640 Å emission line.
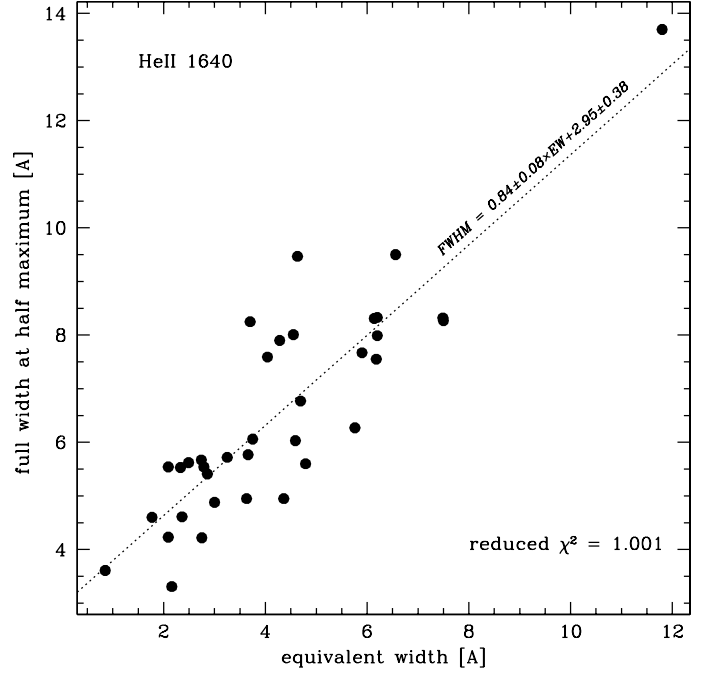
constancy of the continuum (see the SWP spectrum gallery in Fig. 5).

This behavior may cast some doubt on the reality of some emission features, as some of them may be spurious features produced e.g. by cosmic rays hits, due to the long exposure times (more than three hours). A detailed and specific inspection of all the line-by-line (SILO) spectral images has confirmed, however, that several of these features are real emission lines, with only a few being spurious. It is surprising, and somewhat worrisome, that in the extracted spectra of LWP12791 and LWP22052 strong and wide emissions features are present in the region 3100–3250 Å but absent in the SILO image. All SILO images show that the strong Lyα emission is of geocoronal origin, as expected on account of the long exposure times.

Table 4 gives the wavelength and the (tentative) identification for the emission feature considered as real. For many of these emissions the identifications are rather uncertain since they are uncommon in other CVs.

4.2. The features outside the spectrum

It is generally assumed that the shape of the large entrance aperture of the IUE SWP spectrograph is that of a rectangle whose projected size on the camera faceplate has approximate dimensions of 10×20 arcsec. The direction of the dispersion is nearly perpendicular to the major axis of the aperture. Therefore, on the SILO images of an extended object (nebula), one expects to see spectral features on both sides of the star spectrum, out to a distance of ±10 arcsec.

Actually, the IUE large apertures have parallel sides and rounded ends (Bohlin et al. (1980). The full length to the tips of the rounded ends and the width of the SWP's large aperture were measured before flight and the effective dimensions are 23.0×10.3 arcsec. The IUE NEWSIPS manual, Table 2.1 (Garhart et al. 1997) instead gives a large aperture length of 21.65 ± 0.39 arcsec and a large aperture width of 9.07 ± 0.11 arcsec, but the reported large aperture area (215.33 arcsec^2) is quite a bit larger than the product of the quoted length and width, and it is probable that the length does not include the two rounded ends. The precise form and size of the IUE large aperture is apparently not well-defined (see also Gonzalez-Delgado & Perez 2001), but can be considered as intermediate between a rectangle and an ellipse. In the present study we conservatively chose to consider only features at a distance of ≤10 arcsec on either side of the central strip for well-centered objects. The only notable exception is SWP47332 (see below).

The inspection of all SILO images led to the detection of several emission spikes *outside* the central strip of the spectrum but still inside the 20 arcsec large aperture. Some pseudo-emission features are produced by the *permanent* presence of "hot pixels" (for example, a typical one falls near 1750 Å, nearly the same wavelength as a well-known NIII] line, though outside the typical position of well-centered spectra). It is also possible that several of these spikes are caused by cosmic ray hits mimicking the PSF of *IUE*. However, there are cases in which the spikes either are strictly associated with known emission features present in the (main) spectrum or show a common pattern hardly attributable to the impact of cosmic rays.

For example: in SWP49365 a spike at 1243 Å is at the same wavelength as a spectral feature, probably NV 1240; in
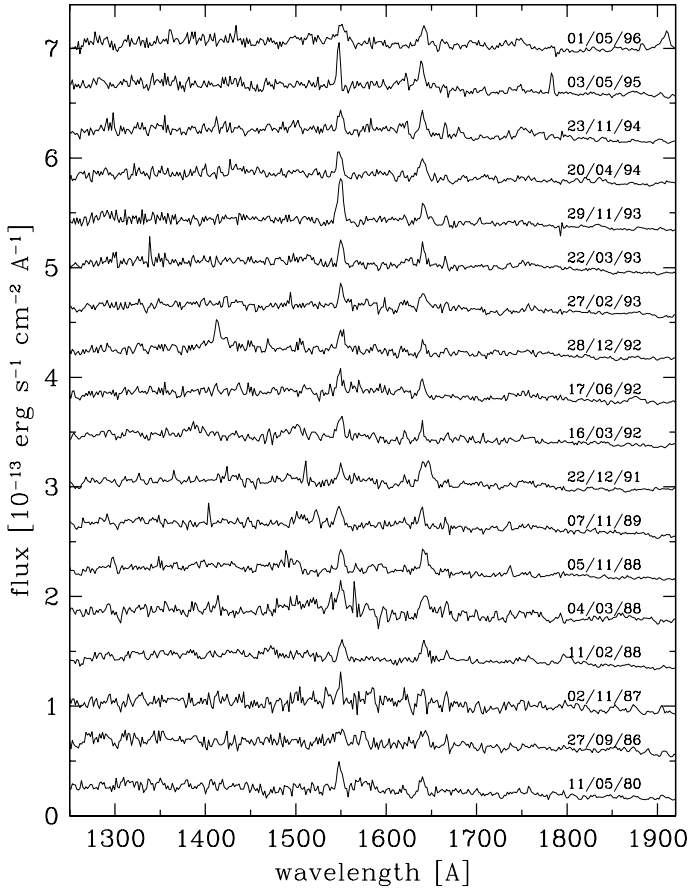
Fig. 5. SWP observed spectra gallery. Spectra are offset by 4×10^{-14} erg s^{-1} cm^{-2} A^{-1}. The near constancy of the continuum contrasts with the changes in the emission lines.

Table 4. Emission lines present only in a few spectra and *not* listed in Table 2.

Wavelength[a]	Identification[b]	SWP spectrum
1190	SIII(1) 90.20	29318, 37536, 44182, 53810, 56240
1243	NV(1) 40.15	49365
1250	CIII(9) 47.38	57039
1285	CI(5) 80.62	56240
1371	OV(7) 71.29	08973
1412	NI(10) 11.97	43442
1474	SI(3,4) 73.77	50596
1713	SiII(10) 11.0	57034
1727	?	53810
1775	?	57039
1782	FeII(191) 85.27	29318,
1890	SiIII(1) 92.03	50099
1910	CIII(0.01) 08.73	08973

[a] The listed wavelength is the mean multiplet wavelength; [b] most identifications are tentative.

SWP43442 a knot at 1414 is at nearly the same wavelength as a spectral feature at 1412 Å; in SWP33034, SWP53809, and SWP47057, there are spikes near 1545 Å that seem associated with CIV 1550; in SWP57055 there are two strong spikes at 1703 and 1873 Å, both lying on the same side of the spectrum, at the *same* distance (about 9 arcsec) from it (see Fig. 6 right; as already mentioned in Sect. 2 they are present as strong emission lines in the INES extracted spectrum and flagged as

"cosmic rays"); the same in SWP54590 at 1751 and 1934 Å; finally in SWP08973 a spike at 1909 Å is associated with an emission feature at 1910 Å on the spectrum (probably CIII] 1909).

The case of SWP47332 is instead quite problematic because there are apparently four spikes near 1640 Å (Fig. 6 left) and also four ones near 1400 Å (not in the same pattern, although one is the same distance from the spectrum at both wavelengths). The two stronger spikes on both sides of HeII 1640 would fall outside the large aperture if one assumes the "standard" 20 arcsec size, but they would fall just near the border if one adopts the 23.0 arcsec size given by Bohlin et al. (1980). A comparison with the spatial size (perpendicular to the dispersion) of the geocoronal Ly-alpha (that fills the large aperture) shows that the separation between the two external features near $\lambda 1640$ is close to the spatial width of the geocoronal Ly-alpha, although the saturation effects in the geocoronal line, together with the difference in the spatial point spread function for the two wavelength regions (Cassatella et al. 1985; Garhart et al. 1997, makes it difficult to make a definite statement about the true nature of the two external features. This particular example highlights the difficulties one encounters in establishing the reality of the "external" features in IUE spectra, especially when nature also maliciously conspires to place two symmetrical knots on either side of a well-known spectral line.

In general, if the external spikes correspond to spectral features, they may originate in the extended region (nebula) surrounding the system, although that only one or, at most, a few external features (and not an entire spectrum of several emission lines) are present in an image is of difficult to explain physically. On the other hand, an examination of the SILOs of other faint emission line objects (Seyfert Galaxies), made for comparison, has not revealed as many spikes features as in T Pyx, although the spectra were taken with similar exposure times.

An analysis of the distribution of spikes inside and outside the large aperture has not been conclusive in demonstrating that the distribution inside is statistically larger than that outside. Apart from small numbers, the probable reason for this is that the background varies substantially in different regions of the image, and even small variations in the threshold (in terms of σ_{bgd}) for automatic spike detection give different results. If one only uses "bright" spikes, the number within the aperture is often larger than that expected from the average in the frame; but this is difficult to quantify in a totally objective way since the "brightness" of the spikes also depends on the position in the frame. Even so, the result for bright spikes, together with the comparison with similarly exposed spectra, would appear a strong argument in favor of at least some of the spikes being real line emissions.

There are however, no obvious, known candidates that would produce spikes near the edge of the aperture. Figure 7 shows the *IUE* aperture during the observations in Fig. 6 superimposed on the HST image of T Pyx and its surroundings (Shara et al., 1997). The aperture is plotted with a standard $10'' \times 20''$ size, although the long axis is probably 15% longer, as explained above. The lack of prominent knots in the shell near the rounded edge of the aperture is not in itself sufficient for excluding the reality of the spikes: the HST image is a composite of observations taken in 1994–95, while the *IUE* observations were taken in 1993 and 1996 and we know that the spikes are short-term transients, e.g. the ones in SWP 57055 were not present a day before in SWP 57047 (although this point may be considered an argument against the interpretation that they are emission lines). The absence of candidates certainly weakens the interpretation that the spikes are emission lines rather than cosmic rays in the
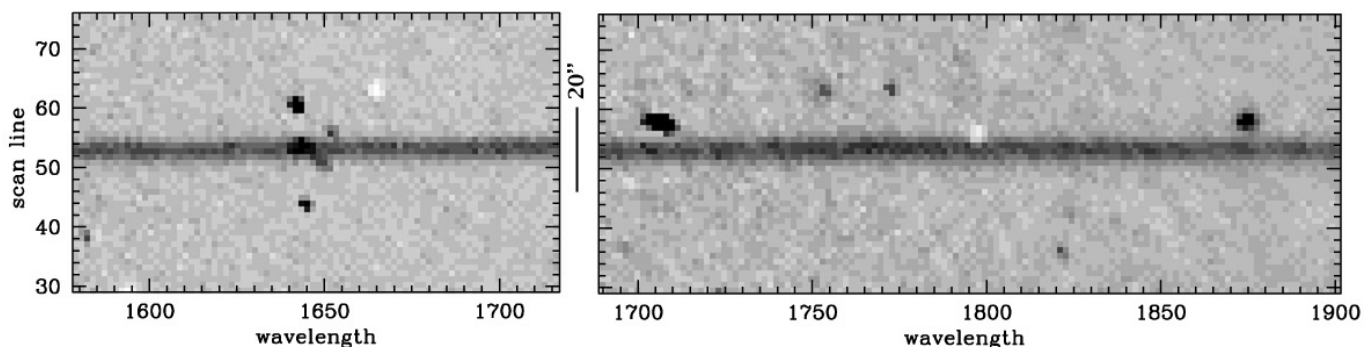
Fig. 6. Line-by-line images of SWP47332 (*left*) and SWP 57055 (*right*). The two symmetrical knots on either side of the HeII 1640 line in the left image fall very near the border of the large aperture. Their reality is uncertain, see the text for details. The bright knots just above the spectrum in the image on the right are those responsible for the emission lines at 1703 and 1873 Å in Fig. 1.
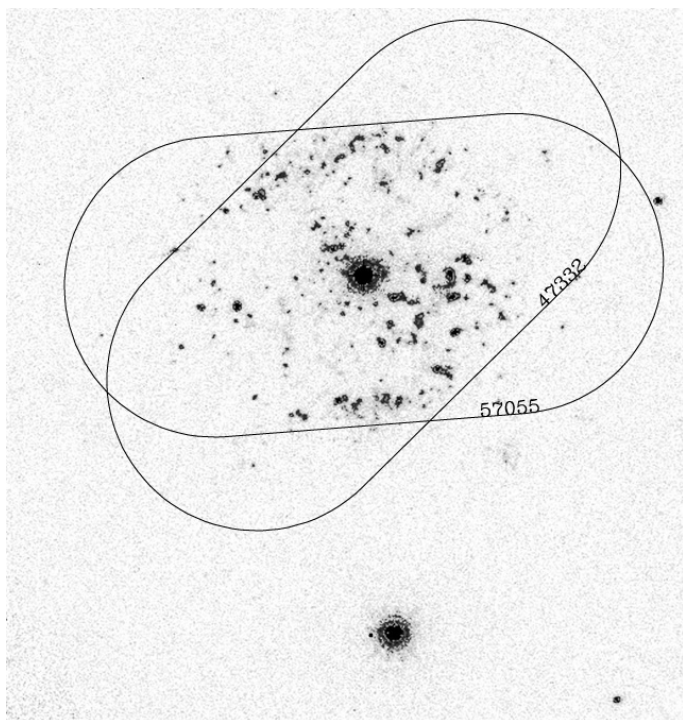

Fig. 7. *IUE* slit position during the observations reported in Fig. 6 superimposed on an HST image of T Pyx and its "shell". The *IUE* aperture is drawn with a size of 10″ × 20″ (tip to tip), although the long axis is probably 15% longer. No obviously bright candidates for the transient features detected in 1993 and 1996 by *IUE* are evident near the edge of the aperture in the composite HST image taken in 1994–1995.

case of SWP 47332. There are instead enough knots at 5–6″ from T Pyx that an origin in the nebula for the spikes in SWP 57055 cannot be ruled out.

5. The absorption lines and the model spectra

In spite of the limited spectral resolution, the good S/N in the average spectrum has allowed positive detection of several absorption features (Fig. 3, top). They are all listed in Table 5, together with their corresponding equivalent widths and the identifications. Most of them are identified as well-known resonance lines of once ionized species.

An interstellar contribution to the zero-volt component in some of these lines is expected, but the presence of intrinsic variations in individual spectra (especially for the SiII 1260 line) and

Table 5. Equivalent widths and identifications for the absorption lines in the average spectrum.

Wavelength	EW [Å]	Identification
1191	0.89	SiII(5) 90.41 + SIII(1) 90.20
1259	1.15	SiII(4) 60.42 + FeII(9) 60.54
		+ SII(1) 59.52
1303	1.01	OI(2) 02.17 + SiII(3) 04.37
1334	0.73	CII(1) 35.10
1371	0.40	NiII(8) 70.20
1529	0.52	SiII(2) 26.71
1628	0.49	?
1727	0.82	?
1807	0.50	SiII(1) 08.01
1816	0.14	SiII(1) 16.92
2376	1.35	FeII(2) 73.73
2475	1.00	TiII(2) 78.64
2600	0.75	Fe II(1) 99.39 + MnII(1) 05.70
2799	1.06	MgII(1) 97.92 +
2853	0.41	MgI(1) 52.12

the weakness of the absorption near MgII 2800 indicate that it is not dominant. Unfortunately, the limited resolution of the *IUE* low resolution spectra has not allowed the intrinsic profile of the lines to be appreciated and the probable presence of more than one contributor to be detected.

It is probable that most of the absorption lines originate in the accretion disk itself. Wade & Hubeny (1998) present a large grid of computed spectra from steady-state accretion disks in luminous CVs. Disk spectra corresponding to twenty-six different combinations of accretion rates and WD masses are computed and tabulated for six different disk inclination angles i. The wavelength coverage of the models ranges from 800 to 2000 Å so it is possible to compare them with the *IUE* spectra taken with the SWP camera (1160–1960 Å). The spectral features we used for the fitting are the intensity and width of the undisplaced absorption lines (e.g. SiII 1260, OI + SiII 1305, CII 1335, etc). Most of the 156 different models were compared with the reddening-corrected average SWP spectrum of T Pyx but, disappointingly, while there is quite a range of values that gives a satisfactory agreement with the observed depth and shape of the absorption lines, no single solution is convincingly valid at the same time both for the continuum distribution and the depth and shape of the absorption lines. The best fits for the shape and depth of the lines (models *ee* and *jj* at rather low inclination angles) correspond to high values for the white-dwarf mass

($M_1 \sim 1.21\ M_\odot$ and $\sim 1.03\ M_\odot$), but give a continuum that is too steep.

6. Discussion

In the following three subsections we will first compare the UV spectrum of T Pyx with that of other ex-novae, then we will suggests some mechanisms to explain the origin of the UV emission lines and their variations, and finally we will consider the origin of the observed optical and IR magnitudes of T Pyx.

6.1. T Pyx and other ex-novae in the UV

We compared the dereddened UV spectrum of T Pyx with all the available IUE spectra of novae in quiescence (about 18 objects, including V603 Aql, RR Pic, HR Del, V533 Her, V841 Oph, etc.).

Surprisingly, the best agreement for the shape of the continuum and the intensity of the emission lines has been found with the very-slow nova HR Del (see also Selvelli & Friedjung, 2003), whose UV spectrum would be almost indistinguishable from that of T Pyx, were it not for the two absorption components in the NV 1240 and CIV 1550 resonance lines that are prominent features in HR Del (Fig. 8). This remarkable similarity in the continua of the two stars is quite a challenge to common interpretations: T Pyx is allegedly observed at rather low inclination ($i \sim 15$–20 degrees) and its WD must be very massive (about 1.2–1.4 $M_\odot$) in order to guarantee outbursts with a very short recurrence time (see also Paper II). HR Del, instead, is observed at medium inclination ($i \sim 45$ degrees) and its WD is allegedly on the light side (about 0.6 $M_\odot$) (see Selvelli & Friedjung 2003, for a discussion on these latter parameters). If we anticipate from Paper II that the accretion rates in the two stars are quite similar, then one would expect a much hotter (steeper) continuum for T Pyx. The fact that T Pyx and HR Del show the same intensity in the HeII 1640 emission line suggests that these (in principle very different) objects also have very similar temperature and continuum distribution in the EUV region, since the 1640 Å line is a recombination line of He^{++}, whose ionization is controlled by the radiation field shortward of 228 Å.

Another peculiarity of T Pyx is its absorption spectrum. Blue-shifted absorptions components in the resonance lines of high ionization species (CIV, SiIV, NV) are generally seen in the UV spectra of luminous (high mass-transfer rate) cataclysmic variables observed at low inclination (e.g. Nova-like, dwarf novae in outburst, the old novae HR Del and V 603 Aql). The absence of any such signature of outflow in T Pyx (which is luminous and observed at low inclination) indicates that at least one basic ingredient for the onset of outflow is missing in this system.

Moreover, the absence in most spectra of T Pyx of both the NV 1240 and the SiIV 1398 resonance lines is also surprising, since these emissions are common in most UV spectra of cataclysmic variables, and, usually, because of their different sensitivity to temperature effects, the absence of one ion is complemented by the presence of the other (while the intermediate temperature ion CIV 1550 always tends to be present). We can tentatively interpret the absence of SiIV as due to a very hot boundary layer whose hard radiation keeps silicon in ionization states higher than Si^{+3}, but in this case it is hard to understand why there is no evidence of the NV 1240 lines either in emission or in absorption.
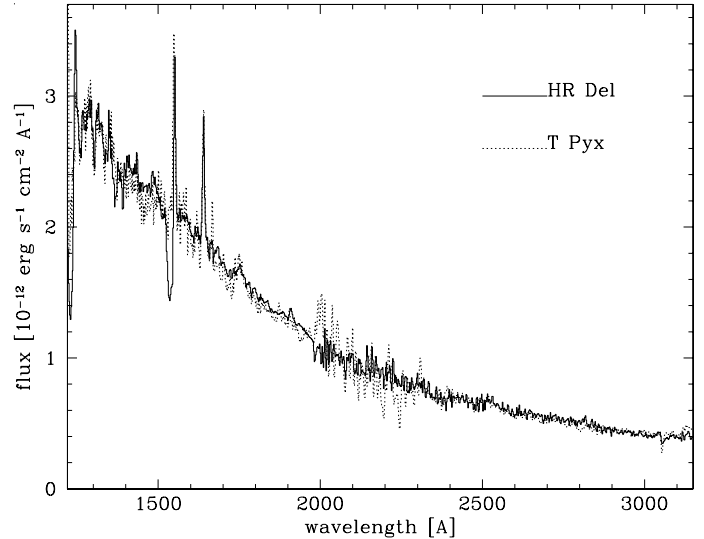

Fig. 8. Comparison between the spectra of T Pyx and HR Del. The two spectra are almost indistinguishable except for the P Cyg component in the CIV 1550 line of HR Del. The spectrum of T Pyx has been scaled to the flux scale of HR Del.

In the old nova V603 Aql, which is observed at almost the same (low) inclination as T Pyx, both NV 1240 (in absorption) and SiIV 1400 (in emission) are present. Also in the old nova RR Pic the line excitation is much higher than in T Pyx: the NV 1240 Å, CIV 1550 Å, and HeII 1640 Å emission lines are much stronger than in T Pyx. This point will be further discussed in Paper II in the context of the alleged SSS nature of T Pyx, as proposed by Patterson et al. (1998).

Common nebular lines (e.g. NIV] 1483, SiIII] 1892, CIII] 1909, etc.) are usually absent in the UV spectrum of T Pyx, in contrast to the presence of a (composite) nebular shell surrounding the central object. It is tempting to explain this with the fact that the nebula has a quite small covering factor because of its knot structure and therefore most of the Lyman continuum radiation of the central hot source leaves the star undisturbed and is not degraded into line radiation (HI emissions plus coolants). However, the presence of conspicuous emission lines of HI and HeII casts some doubts on this interpretation. Another possibility is that the near absence of nebular lines could simply be a density effect, the knots' condensations having electron densities higher than the critical ones for the relevant emission lines.

6.2. Speculations on the origin of the UV emission lines and their variations

The emission line spectrum of T Pyx shows some peculiarities whose interpretation is not straightforward:

1. the strongest emission lines (CIV 1550, HeII 1640) are variable in intensity and width;
2. some lines are observed in a few spectra only and are uncommon in CVs and/or lack reliable identification;
3. some lines appear inside the slit (not on the spectrum) at uncommon wavelengths and varying positions.

The observed emission-line variations, which in some cases take place on time scales as short as a few hours (see the spectra taken in sequence in May 1996), are not caused by instrumental effects, i.e. different centerings in the *IUE* aperture that could produce different contributions from the nebular shell. In all the

SILO images we have examined (with the few exceptions mentioned in Sect. 4.2), there was no evidence of any contribution from an extended region.

The *IUE* Roll angle (which determines the slit's position angle) is fixed during one exposure, but varies at different epochs. Therefore, knots that may be in the 10×20 arcsec aperture at one epoch may not be at another, although knots within 10 arcsec of the star are always in the aperture. Even for these, at different position angles the same knot will produce lines that are not only at a different distance from the main spectrum (or even *on* it) but also at different wavelengths from epoch to epoch (up to ± 8 Å depending on the geometry inside the slit). This may help explain the sporadic appearance of lines on and outside the spectrum but, of course, not the variations of the known lines.

Also, the variations can hardly be ascribed to aspect-dependent and/or orbital and geometrical effects (bulges, hot spots, etc.) because the system is allegedly viewed nearly pole-on ($i \leq 20°$, Paper II) and the average exposure time of all spectra is longer than the orbital period so that orbit-dependent effects should be averaged over one orbital period or more. The observed variations in the lines of the spectrum must take place in a region whose angular size is on the order (or less) of the PSF of *IUE* ($\leq 2.7\,''$). This region contains the binary system and the innermost nebula (and that part of the nebula that is projected on the compact source).

In other CVs, intrinsic variations in the emission lines are observed in systems that are not stable accretors (e.g., dwarf novae from low to high states, etc.) when they suffer $\dot{M}$ changes in an optically thin accretion regime. This is apparently not the case for T Pyx. The high luminosity of the UV continuum, remarkably constant over 16 years, indicates stable accretion in an optically thick regime.

Besides the difficulty of explaining the variations, the problem also remains with the unidentified or poorly identified features. It is probable that these emission lines may come from regions other than the hot component (accretion disk plus boundary layer), so we tentatively suggest these non mutually-exclusive regions and/or mechanisms:

1) The (irradiated) chromosphere of the M dwarf companion.

Several short-period detached binary systems are known - e.g.: V471 Tau (Guinan 1990; Young et al. 1988), BE UMa (Ferguson et al. 1991), Feige 24 (Vennes et al. 1991) – which show irradiation induced effects: the atmosphere of the companion star, usually a low-MS star, is heated by the flux of the WD leading to an enhancement of line emission. These systems are thought to be pre-cataclysmic binaries (de Kool & Ritter 1993); see also Jomaron et al. (1993). In some of these systems, e.g. V471 Tau, the atmosphere of the K star is inhomogeneous and there is evidence of external plasma around it (Young et al. 1991; Guinan 1990). These atmospheric structures may be related to the cool loops or active region plumes observed in the Sun, but are much more extensive in size and are unstable, with a lifetime of a few days.

We suggest that a similar class of phenomena could also be present in T Pyx, where transient jets or loops from the cool star, excited by the strong UV radiation of the hot component, may be responsible for the variations and peculiarities of its spectrum. However, while the above-mentioned objects are semi-detached binaries in which the luminosity and temperature of the WD is not particularly high, T Pyx is instead a short-period semi-detached system with high ultraviolet luminosity ($L_{\rm UV} \sim 100\,L_\odot$, Gilmozzi et al. 1998; and Paper II) and

rather high average T ($\sim 34\,100$ K), so that much stronger induced effects are expected. Urban (1988) has already pointed out the importance of irradiation effects on the spectrum of T Pyx.

2) The enhanced activity in the secondary and magnetism.

It is well-known that most M dwarfs are characterized by a surface magnetic activity that is manifested by non thermal emission in a hot outer atmosphere (see Hawley 1993, for a review). The magnetic activity increases monotonically toward later spectral types, until at type M 5 and later all dwarfs are dMe or active and show high-temperature UV emission lines. Rotation also plays an important role in this class of phenomena, therefore, it is possible that binarity with a close companion might increase these effects by tidally-induced rapid rotation, together with irradiation and heating. Flare activity is associated with phenomena like coronal loops and coronal mass ejection that have sizes on the order of the stellar radius and time scales on the order of hours (see the observations of AU Mic with EUVE by Katsova, 1996). Also, if the WD in T Pyx is mildly magnetic, the two stars are probably interconnected by a magnetic field that acts as a guide line for the material streaming from the secondary, and the interaction of the two magnetic fields may heat the plasma between the two stars. A representative spectrum of an active star (AD Leo) is given in Fig. 3 (bottom); the three strongest emission lines are those of CIV $\lambda1550$, HeII $\lambda1640$, and OIII $\lambda1660$, with relative intensities similar to those observed in T Pyx.

In the context of these two models, the absence in the UV spectrum of T Pyx of the MgII 2800 emission line, a well-known indicator of chromospheric activity, is quite disturbing. We can only invoke the somewhat *ad hoc* explanation that the MgII emission is suppressed by the corresponding absorption component of the accretion disk and by the interstellar medium.

3) Illumination of (moving) knots of the nebula in front of the compact object.

Shara et al. (1997) report that a few knots are observed to fade or brighten significantly on a timescale of months and interpreted this in terms of collisions and shocks between successive generations of ejecta. From the comparison of the size of the nebula at different epochs, they derived an upper limit of about only 40 km s^{-1} (but assumed d = 1500 pc) on the systematic expansion velocity of the knots. Instead, both Margon & Deutsch (1998) and O'Brien & Cohen (1998), in a study of the alleged jet components in the Hα line (Shabaz et al. 1997), identified these features as due to the [NII] 6548, 6584 lines and interpreted their wavelength shifts as produced by an expansion velocity of about 500 km s^{-1} along the line of sight through the center of the shell. If some of these "variable knots" happen to lie within the *IUE* PSF they may also explain the emission line changes and the unusual spectroscopic signatures in the UV spectrum of T Pyx.

To summarize this rather speculative section, we propose that the peculiar spectrum of T Pyx may be due to complex velocity fields in the material (cool loops, active region plumes, transient jets, coronal loops, etc.) that streams from the active companion toward the WD and/or to the transient appearance of high-velocity emitting knots in front of the compact object. That in individual UV spectra only a few extra emission lines (most of them of dubious identification) are observed, instead of a spectrum, means that interpretation is difficult and that quite uncommon physical conditions are required.

The data we have are too sparse to test other possible effects contributing to the unusual behavior of T Pyx. For
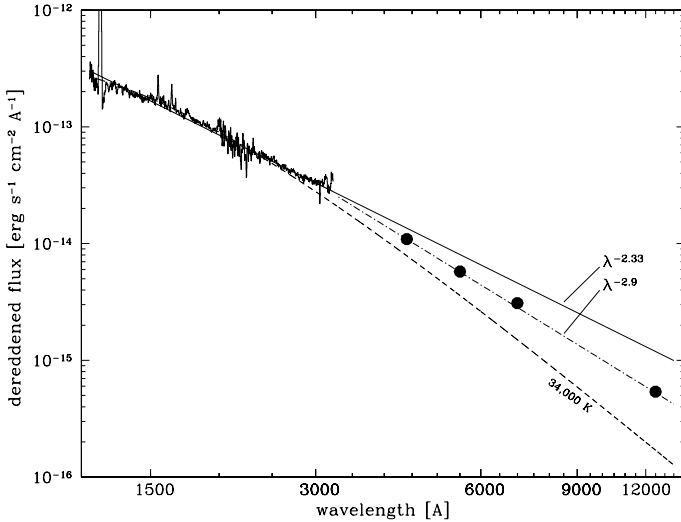
Fig. 9. UV-Opt-IR "spectrum" of T Pyx. The B, V, R, J average fluxes are indicated. The hot source is clearly the main contributor at all wavelengths (the departure from the -2.33 power-law at long wavelengths probably indicates that these fluxes arise in the outer part of the disk, where it becomes optically thin or reaches a physical edge). The $\alpha = -2.9$ power-law is an aid to the eye. The black body that best "fits" the UV continuum (though meaningless for an accretion disk) is also plotted.

example, we have considered precession in the system (partially) hiding and revealing at different epochs a possible hot spot as one explanation for the variability in the emission lines, but much more intensive observations would be necessary to test this hypothesis.

We also considered other more "exotic" scenarios in view of the peculiarities of T Pyx, for instance, that some of the uncommon, sporadic lines may be typical lines that are blue- or red-shifted in a jet. But apart from the occasional, correct wavelength ratio between lines being similar to that of HeII/CIV or NIII]/HeII (at a few to several thousand km s^{-1}), there is little evidence to support this hypothesis.

6.3. The origin of the optical and IR magnitudes

The extrapolation to the V band of the power-law fit of the UV continuum $F_\lambda = 4.28 \times 10^{-6} \lambda^{-2.331}$ erg cm^{-2} s^{-1} A^{-1} yields a flux $F_{5500} = 8.17 \times 10^{-15}$ erg cm^{-2} s^{-1} A^{-1} or $m_{\rm v} \sim 14.10$. After proper reddening with $A_{\rm v} = 0.78$, the predicted V magnitude is 14.88. Similar calculations for the B band yield a flux $= 1.34 \times 10^{-14}$ erg cm^{-2} s^{-1} A^{-1} or $m_{\rm b} \sim 14.23$. After reddening using $A_B = 4.1 \times E_{B-V} = 1.03$, this becomes $B = 15.26$. Therefore, the observed $B = 15.5$ (Schaefer (2005) and $V = 15.3$ (Downes et al. 1997; Szkody & Feinswog 1988) magnitudes of T Pyx fall quite close to the values defined by the tail of the power-law fit to the UV continuum. This indicates that m_B and m_V are dominated by the hot component (accretion disk). That the extrapolated $B - V$ value (after reddening) is close to 0.38 and larger than the observed one (close to 0.20) is due to the fact that the spectrum departs from the power-law extrapolation at longer wavelengths (see below and Fig. 9).

The extrapolation to 12 500 Å (J band) gives 1.20×10^{-15} erg cm^{-2} s^{-1} A^{-1}. After conversion to J magnitudes and reddening with $A_J = 0.87 \times E_{B-V} = 0.22$, we obtain $J = 13.52$, to be compared with the observed $J = 14.4$–14.65 (Szkody & Feinswog 1988; Weight 1994) Therefore also in the J band, it is

the IR tail of the hot source that is the main contributor to the observed magnitude.

This progressive departure from the power-law distribution is most probably an indication that the largest contribution of the disk to these wavelengths comes from its outer region, where it becomes optically thin (or reaches a physical edge). With a full spectral coverage, it should be possible to determine the temperature of this region. Judging from the optical and infrared colors, this should not be far from 10 000 K.

Szkody & Feinswog (1988) found a sinusoidal modulation in the J light curve of T Pyx from $J = 14.34$ to $J = 14.50$ with $P = 100$ min (single sine solution) or $P = 200$ min (double sine solution), which was interpreted as due to ellipsoidal variations in the secondary, that, allegedly, provided a substantial contribution to the IR light. They then applied the technique of ellipsoidal fitting to derive the system inclination (close to 90 degrees) and the mass ratio q (close to 4).

This interpretation, however, is compatible with the observations only if the distance to T Pyx is quite low (and they actually suggested a value close to 350 parsecs). In fact, from various relations available in the literature between M_J and other stellar parameters such as the mass, the spectral type, etc. (Henry & Mc Carthy 1990; Henry & Mc Carthy 1993) or from the observed J values for objects in clusters with known distances (Legget & Hawkins 1989), it follows that the M 4–M 5 V secondary star in T Pyx (see the Introduction) has an absolute magnitude $M_J \sim 7.8$ (or dimmer). This value, together with the observed $J \sim 14.5$, and $A_J = 0.22$ would imply a distance to T Pyx of only 198 pc (or smaller), not compatible with any value reported in the literature whose lower limit is about 1050 pc (Shara 1997), while a value near 3500 pc is the most plausible (see Paper II). If the largest value is correct, the apparent J magnitude of the secondary star would be about 20.7, and would thus contribute to less than 1 percent of the observed J flux.

Therefore the IR tail of the hot source is the main contributor to the observed $J = 14.4$ mag. It is possible, however, that heating (irradiation) of the secondary by the accretion disk (see Sect. 6.2) could provide a partial contribution to the J light and be responsible for its modulation. In any case, the presence of a definite modulation in the J curve and the absence of a similar modulation in the optical, where several photometric periods have been reported, are difficult to interpret if, allegedly, the system is seen at the inclination of ~ 15 degrees (Warner 1995).

7. Conclusions

The constancy of the UV continuum energy distribution over 16 years of *IUE* observations is quite remarkable in an object that belongs to the CVs class. This behavior contrasts with the observed changes both in intensity and detectability for the UV emission lines. The strongest emission lines (CIV 1550 and HeII 1640) are clearly variable in intensity and width.

The origin of these variations is unclear, so we suggest that the peculiar behavior of T Pyx may be due either to complex velocity fields in the material that streams from the active companion toward the WD (cool loops, active region plumes, transient jets, coronal loops, etc.) and/or to the transient appearance of high-velocity emitting knots from the nebular shell in front of the compact object.

The best single-curve fit to the dereddened ($E_{B-V} = 0.25 \pm 0.02$) UV continuum is a power-law distribution $F_\lambda = 4.28 \times 10^{-6} \lambda^{-2.33}$ erg cm^{-2} s^{-1} A^{-1}, with a small uncertainty of ± 0.04 in the index. The observed $B = 15.5$, $V = 15.3$, and $J = 14.4$ mag of T Pyx fall quite close to the values defined by the tail of this

power-law. This clearly indicates that the hot source (accretion disk) is the main contributor at all wavelengths and that the contribution from the secondary star is negligible, also in the IR.

References

Bohlin, R. C., Sparks, W. M., Holm, A. V., Savage, B. D., & Snijders, M. A. J. 1980, A&A, 85, 1
Bruch, A., Duerbeck, H. W., & Seitter, W. C. 1981, Mitt. Astr. Ges., 53, 34
Bruch, A., & Engel, A. 1994, A&AS, 104, 79
Cassatella, A., Barbero, J., & Benvenuti, P. 1985, A&A, 144, 335
de Kool, M., & Ritter, H. 1993, A&A, 267, 397
Downes, R., Webbink, R. F., & Shara, M. M. 1997, PASP, 109, 345
Duerbeck, H. W. 1987, Space Sci. Rev., 45, 1
Duerbeck, H. W., & Seitter, W. C. 1979, The Messenger, 17, 1
Garhart, M. P., Smith, M. A., Turnrose, B. E., Levay, K. L., & Thompson, R. W. 1997, IUE NASA Newsletter, 57, 1
Gilmozzi, R., Selvelli, P., & Cassatella, A. 1998, in Ultraviolet Astrophysics Beyond the Final Archive, ESA-SP, 413, 415
González Delgado, R. M., & Pérez, E. 2000, MNRAS, 317, 64
Gonzalez-Riestra, R., Cassatella, A., & Wamsteker, W. 2001, A&A 373, 730
Guinan, E. F. 1990, in Evolution in Astrophysics, ESA-SP, 310, 73
Hawley, S. L. 1993, PASP, 105, 955
Henry, T. J., & Mc Carthy, D. W. 1990, ApJ, 350, 334
Henry, T. J., & Mc Carthy, D. W. 1993, AJ, 106, 773
Katsova, M. M., Drake, J. J., & Livshits, M. A. 1996, in Astrophysics in the EUV, ed. S. Bowyer, & R. F. Malina (Kluwer Acad. publ.), IAU Coll., 152 175
Kemp, J., Shambrook, A., Patterson, J., et al. 1998, PASP, 110, 380
Krautter, J., Beuermann, K., Leitherer, C., et al. 1984, A&A, 137, 307
Landolt, A. U., Vogt, N., Schaefer, B. E., et al. 1992, ApJS, 81, 321
Legget, S. K., & Hawkins, M. R. S. 1989, MNRAS, 238, 145
Liebert, J., Cutri, R., Ferguson D. H., et al. 1987, ApJ, 316, 399
Margon, B., & Deutsch, E. W. 1998, ApJ, 498, L61
O'Brien, T. J., & Cohen, J. 1998, ApJ, 498, L59
Payne-Gaposchkin, C. 1957, The Galactic Novae, North Holland
Raymont, G. B., Bromage, G. E., Jomaron C. M., et al. 1993, MNRAS, 264, 219
Rodriguez-Pascual, P. M., Gonzalez-Riestra, R., Schartel, N., & Wamsteker, W. 1999, A&A, 139, 183
Saizar, P., & Ferland, G. J. 1994, ApJ, 425, 755
Savage, B. D., & Mathis, J. S. 1979, ARA&A, 17, 73
Schaefer, B. E. 2005, ApJ, 621, L53
Schartel, N., & Skillen, I. 1998, in Ultraviolet Astrophysics Beyond the Final Archive, ESA-SP, 413, 735
Seitter, W. C. 1986, in RS Ophiuchi, ed. M. F. Bode (VNU Press), 63
Selvelli, P., & Friedjung, M. 2003, A&A, 401, 297
Selvelli, P., & Gilmozzi, R. 2006, in preparation (Paper II)
Shahbaz, T., Livio, M., Southwell, M., & Charles, P. A. 1997, ApJ, 484, L59
Shara, M. M., Moffat, A. F. J., Williams, R. E., & Cohen, J. C. 1989, ApJ, 337, 720
Shara, M. M., Zurek, D. R., Williams, R. E., et al. 1997, AJ, 114, 258
Shore, S. N., Sonneborn, G., Starrfield, S., Riestra-Gonzalez, R., & Ake, T. B. 1993, AJ, 106, 2408
Smith, D. A., & Dhillon, V. S. 1998, MNRAS, 301, 767
Szkody, P. 1994, AJ, 108, 639
Szkody, P., & Feinswog, L. 1988, ApJ, 334, 422
Urban, Z. 1988, in Eruptive Phenomena in Stars Comm. Konkoly Obs., Acad. Sci., 86, 359
Vennes, S., Thorstensen, J. R., Thejll, P., & Shipman, H. L. 1991, ApJ, 372, L37
Vogt, N., Barrera, L. H., Barwig, H., & Mantel, K. H. 1989, in Accretion-Powered Compact Binaries, ed. C. W. Mauche (Cambridge Univ. Press), 391
Wade, R. A., & Hubeny, I. 1998, ApJ, 509, 350
Warner, B. 1995, in Cataclysmic Variable Stars (Cambridge Univ. Press)
Webbink, R. F., Livio, M., Truran, J. W., & Orio, M. (WLTO) 1987, ApJ, 314, 653
Weight, A., Evans, A., Naylor, T., Wood, J., & Bode, M. F. 1994, MNRAS, 266, 761
Williams, R. E., Hamuy, M., & Phillips, M. M. 1991, ApJ, 376, 721
Young, A., Skumanich, A., & Paylor, V. 1988 ApJ, 334, 397
Young, A., Rotler, L., Skumanich, A., et al. 1991, ApJ, 378, L25